J. Am. Ceram. Soc., **91** [3] 860–864 (2008)
DOI: 10.1111/j.1551-2916.2007.02224.x

Formation Process of Calcium-α SiAlON Hollow Balls Composed of Nanosized Particles by Carbothermal Reduction–Nitridation

Mikinori Hotta,[†,‡] Junichi Tatami, Katsutoshi Komeya, Cheng Zhang,[§] and Takeshi Meguro

Graduate School of Environment and Information Science, Yokohama National University, Yokohama 240-8501, Japan

Mark R. Terner and Yi-Bing Cheng

Department of Materials Engineering, Monash University, Melbourne, Vic. 3800, Australia

Carbothermal reduction–nitridation (CRN) of SiO_2–Al_2O_3–CaO powders was performed under various firing conditions to investigate the formation process of Ca-α sialon hollow balls composed of nanosized particles. Scanning electron microscopy and transmission electron microscopy observations of the samples obtained at different firing temperatures confirmed that solid spherical particles were formed at the early stage of the reaction, and nanosized particles were subsequently produced on the surface of these solid balls. From X-ray diffraction and energy-dispersive spectrometry analyses, it was found that the solid balls initially formed at 1450°C were mainly amorphous and contained Si, Al, Ca, O, and a small amount of N. Further nitridation at 1450°C gradually converted the solid balls into Ca-α sialon hollow balls over time. The results revealed that the formation of Ca-α sialon hollow balls depends on the formation of solid balls from the Si–Al–Ca–O liquid phase at the initial stage of the CRN process.

I. Introduction

Sialon ceramics are of interest for engineering applications, particularly in severe environments, because they have high hardness and excellent wear and corrosion resistance.[1–5] α-Sialon is isostructural with α-Si_3N_4, and can be represented by the general formula $M_{m/v}Si_{12-(m+n)}Al_{(m+n)}O_nN_{16-n}$, where M is a metal such as Li, Mg, Ca, or most rare earth elements, and v is the valency of the metal cation. In general, α-sialon is produced from Si_3N_4–AlN–M_xO_y powder mixtures at high temperatures via a liquid-phase sintering process.[1–4,6,7] However, because the phase reactions are complex and strongly dependent on the characteristics of the raw powders, it is difficult to fabricate sialon ceramics with homogeneous composition and microstructures through reaction sintering. One method to improve the reliability of sialon ceramics is to develop homogeneous and fine sialon powders using novel processes. Carbothermal reduction–nitridation (CRN) of silicate-based oxides together with carbon in flowing N_2 gas has been used to synthesize many sialon powders, such as β-sialon powder from halloysite ($Al_2Si_2O_5(OH)_4$),[8] kaolinite ($Al_2Si_2O_5(OH)_4$),[9] SiO_2–$Al_2O_3 \cdot H_2O$,[10] SiO_2–Al_2O_3 powder mixtures,[11] alkoxide-derived SiO_2–Al_2O_3 coprecipitate,[12] a SiO_2–Al_2O_3 mixture obtained via sol–gel method,[13,14] and zeolite.[15] Furthermore, α-sialon powder has been prepared by heating carbon-containing mixtures of SiO_2–Al_2O_3–(Ca- or Y-) oxide,[16,17] clay–metal compounds,[18] or talc ($Mg_3Si_4O_{10}(OH)_2$)–halloysite clay minerals[19,20] and slag–clay mixtures.[21,22]

Here, the synthesis of Ca-α sialon powders was performed by CRN of a SiO_2–Al_2O_3–$CaCO_3$ powder mixture. It was found that the Ca-α sialon powders synthesized at 1450°C for 120 min had a hollow ball morphology composed of large numbers of nanosized particles.[23] Such a hollow ball morphology has not been previously reported from CRN investigations; hence it would seem that the formation mechanism for α-sialon is related to the raw materials used.

This outcome may provide a possibility of producing dense sialon ceramics consisting of nanosized grains, or producing porous sialon ceramics by maintaining the hollow ball morphology.[5,24] This paper details the formation process of Ca-α sialon hollow balls composed of nanosized particles during CRN of the SiO_2–Al_2O_3–CaO system.

II. Experimental Procedure

In previous work it was found that the maximum Ca-α sialon content and hollow ball morphology occurred with the starting composition $Ca_xSi_{12-3x}Al_{3x}O_xN_{16-x}$ ($x = m/v = n$) with $x = 1.0$.[23] Hence this composition was studied in the present work.

The starting powders used in this study were SiO_2, Al_2O_3, $CaCO_3$, and carbon black as a reducing agent. Typical characteristics of these powders are summarized in Table I. These powders were of high purity, and both SiO_2 and carbon powders consisted of very fine, amorphous particles. $CaCO_3$ in the mixture decomposes above 900°C to produce CaO and CO_2. The proportions of the raw powders were calculated to give a nominal composition of $Ca_{1.0}Si_{9.0}Al_{3.0}O_{1.0}N_{15.0}$. The expected overall reaction during CRN is described as follows:

$$\begin{aligned}&1.0CaO + 9.0SiO_2 + 1.5Al_2O_3 + 22.5C + 7.5N_2\\&\quad\rightarrow Ca_{1.0}Si_{9.0}Al_{3.0}O_{1.0}N_{15.0} + 22.5CO\end{aligned} \tag{1}$$

The content of carbon powder was fixed to 1.2 times the required stoichiometric value according to Eq. (1). In our

Table I. Characteristics of Raw Powders

Raw powders	Particle size (μm)	Specific surface area (m^2/g)	Purity (%)	Suppliers
SiO_2	0.005–0.05	208	>99.9	Tokuyama, QS-102
Al_2O_3	0.21	10.4	>99.99	Sumitomo Chemical, AKP-50
$CaCO_3$	1.0	1.3	>99.0	Junsei Chemical
C	0.018	>200	>99.97	Mitsubishi Chemical, #650B

K. Watari—contributing editor

Manuscript No. 23517. Received July 27, 2007; approved November 2, 2007.

This work was performed as JSPS Research Fellow (No. 00055) and was supported by JSPS as part of Research for the Future Program and NEDO as part of Synergy Ceramics Project under the ISTF Program promoted by AIST.

[†] Author to whom correspondence should be addressed. e-mail: hotta@imr.tohoku.ac.jp

[‡] Present address: Institute for Materials Research, Tohoku University, Sendai 980-8577, Japan.

[§] Present address: Department of Materials Engineering, Shanghai Institute of Technology, Shanghai 200233, China.

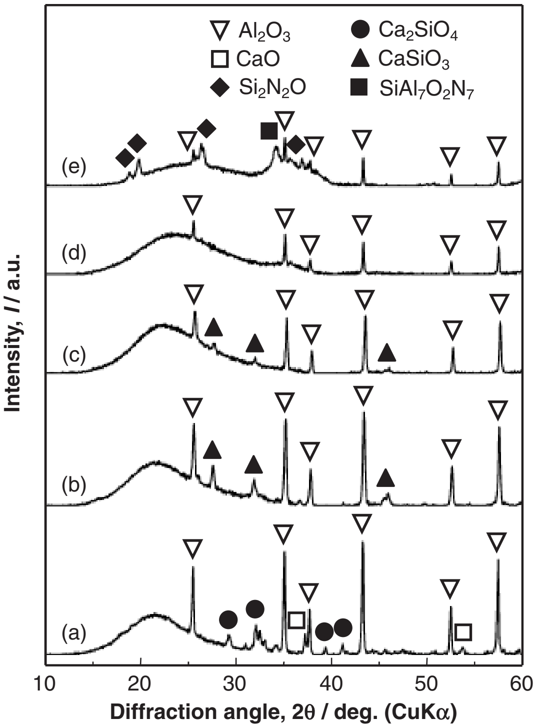

Fig. 1. X-ray diffraction patterns of the products fired at (a) 1100°, (b) 1200°, (c) 1300°, (d) 1400°, and (e) 1450°C for 0 min in N_2 flow.

previous study on the synthesis of Ca-α sialon powders with different amounts of carbon in starting materials, it was found that when a stoichiometric amount of carbon was used, Si_2N_2O, AlN, and $SiAl_7O_2N_7$ were identified as major phases, and Ca-α sialon was a minor phase. The formation of these high oxygen-containing phases indicates that full conversion to Ca-α sialon by CRN process requires more carbon. The use of excessive amounts of carbon was also reported in the synthesis of Si_3N_4 powder from SiO_2 and Mg-α sialon powder from talc–halloysite clay minerals via CRN process.[25,20] The raw powders were mixed with ethanol in an agate mortar for 60 min, dried, ground, and passed through a 300 μm sieve. The powder mixture was placed in a graphite crucible and fired in a horizontal electrical furnace at temperatures ranging from 1100° to 1450°C for different soaking times of 0–120 min. High-purity nitrogen gas (99.999%) with a constant flow rate of 0.5 L/min was employed during the whole heating cycle. The heating rate was 10°C/min. Any residual carbon was removed by firing the reacted powders at 700°C for 120 min in air.

The crystalline phases in the products fired at 1100°–1450°C for 0 min were identified by X-ray diffraction using a 15 kW generator with rotating anode (XRD; RINT-2500, Rigaku Co., Tokyo, Japan) to investigate the process of production of Ca-α sialon at the initial stage of CRN. Particle morphology of resultant powder at 1100°–1450°C for 0 min was characterized by scanning electron microscopy (SEM; JSM-5200, JEOL Ltd., Tokyo, Japan). And further observation using field emission scanning electron microscopy (FESEM; JSM-6340F, JEOL Ltd.) and transmission electron microscopy (TEM; JEM 2000FXII, JEOL Ltd.) was performed on the synthesized powders at 1450°C for 0–120 min. An energy-dispersive spectrometer (EDS) installed on the TEM was used to determine elemental distribution in the powder obtained at 1450°C for 0 min.

III. Results and Discussion

XRD patterns of the products fired at different temperatures and held for 0 min are shown in Fig. 1. At 1100°C both CaO and Ca_2SiO_4 derived from decomposition of the $CaCO_3$ were identified together with Al_2O_3 from the raw powder. In addition, the broad hump observed at low 2θ angles implies the existence of an amorphous SiO_2 phase corresponding to the raw powder. The peak intensities of Al_2O_3, CaO, and calcium silicates significantly decreased with increasing temperature, and by 1400°C all crystalline phases except Al_2O_3 had disappeared, with only the amorphous hump detected at $\sim$25°. This suggests that the amorphous phase contains not only SiO_2 but also Al_2O_3 and CaO, further evidence of which is found in the TEM analysis described later. When the firing temperature was increased to 1450°C, the intensity of Al_2O_3 and the amorphous hump decreased, with Si_2N_2O and $SiAl_7O_2N_7$ phases now being detected. These oxynitride phases may be devitrification products from the nitrogen-containing liquid phase on cooling.[26] These intermediate phases were not seen in previous work when Ca-α sialon was prepared via CRN, where SiO_2 and mullite were

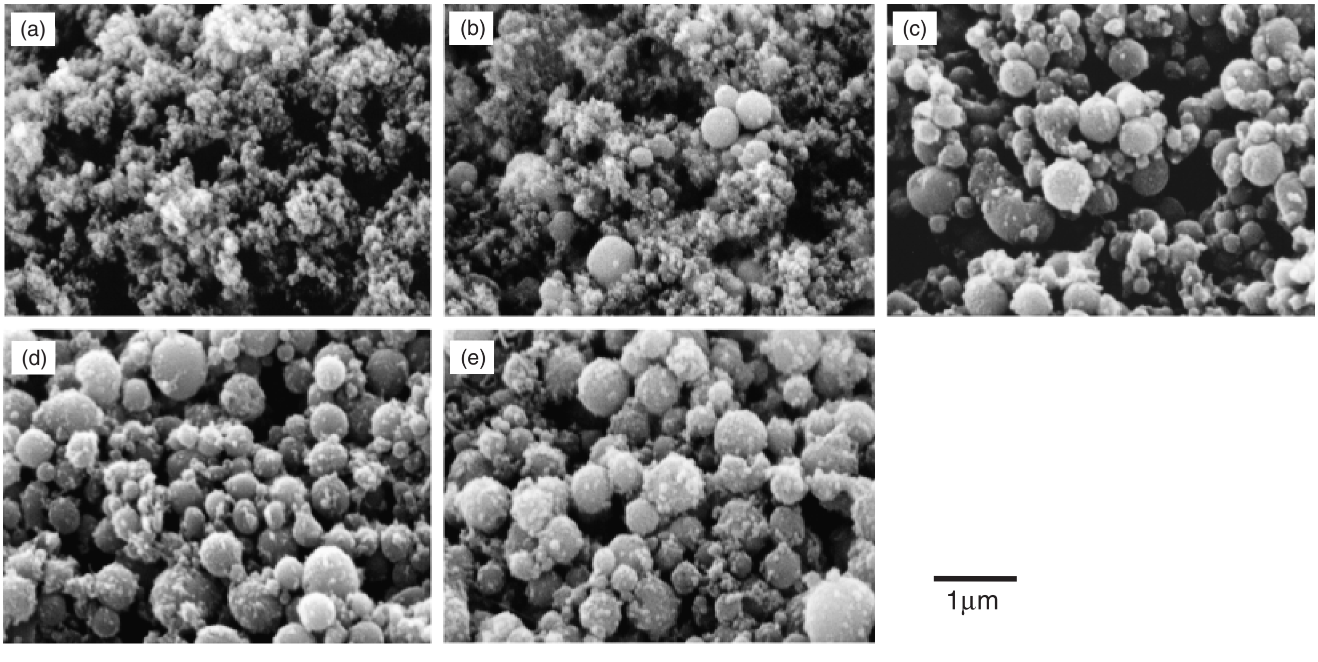

Fig. 2. Scanning electron micrographs of the products fired at (a) 1100°, (b) 1200°, (c) 1300°, (d) 1400°, and (e) 1450°C for 0 min in N_2 flow.

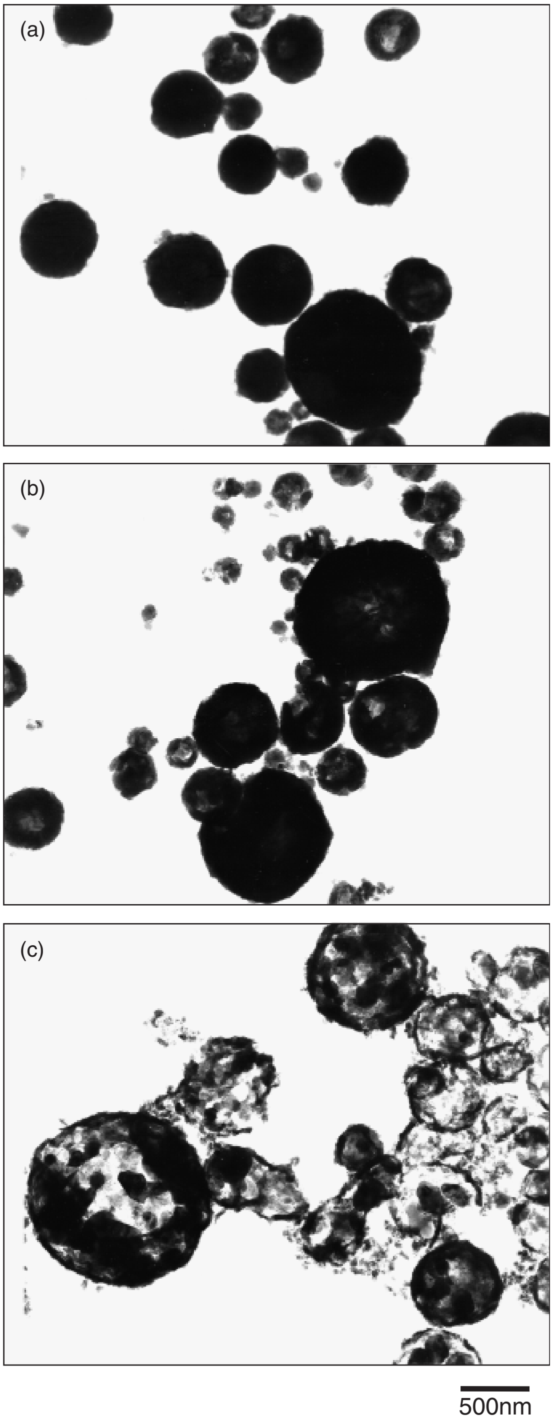

Fig. 3. Transmission electron micrographs of the products fired at 1450°C for (a) 0, (b) 30, and (c) 120 min in N_2 flow.

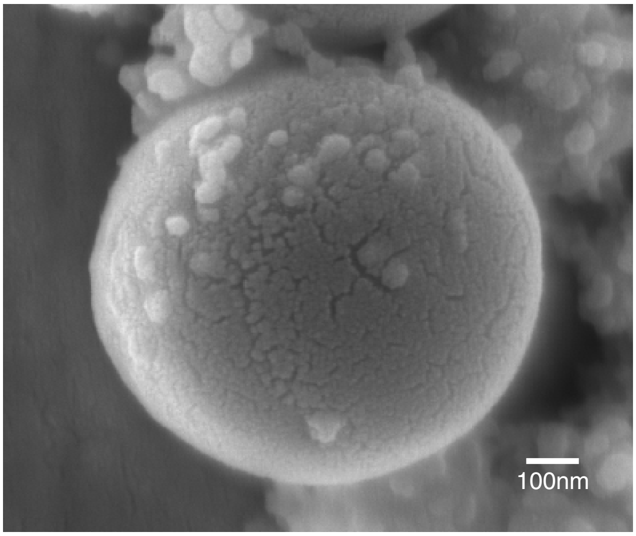

Fig. 4. Field emission scanning electron micrographs of the products fired at 1450°C for 0 min in N_2 flow.

the only crystalline phases found below 1250°C.[16,17] It seems that the formation of Ca-α sialon hollow balls requires the formation of solid amorphous balls from the Si–Al–Ca–O liquid phase at the early stage of the CRN process. The subsequent CRN reaction would convert the solid balls to the spherical hollow morphology containing Ca-α sialon nano particles.

SEM micrographs of the resultant powders after firing at various temperatures and holding for 0 min are shown in Fig. 2. It was observed that the morphologies of the products fired at 1100°C were basically unchanged from the starting powder, but a few spherical particles <0.5 μm diameter were produced at 1200°C. These spherical particles can be attributed to a Si–Al–Ca–O liquid phase that formed above the SiO_2–Al_2O_3–CaO eutectic temperature of 1170°C.[27] The spherical particles seem to be formed due to high surface tension of the liquid. The relatively high viscosity of the liquid phase at this firing temperature restricted the spherical amorphous particles to localized regions and of fine size. The synthesis of Ca-α sialon was also performed using crystalline and coarse SiO_2 particles, and similar spherical solid particles to those obtained in this work were generated at the initial stage of the CRN process. It becomes evident from the SEM observations that the number and size of the spherical particles increased when further increasing the firing temperature due to a significant increase in the size of the liquid phase region in the SiO_2–Al_2O_3–CaO system above 1300°C.[27]

Significant morphological changes were observed by TEM in the samples fired at 1450°C for 0, 30, and 120 min, respectively (Fig. 3). It was clear that the morphology of the particles changed from dark to transparent spheres with increasing soaking time. Therefore, it revealed that with increasing soaking time the solid balls gradually changed into hollow balls, while maintaining their spherical shape and size. After heating to 1450°C for 0 min, it is clear that almost the entire sample was converted into solid balls with only a few hollow balls present. A significantly larger number of hollow balls were observed in the products after 30 min compared with 0 min. After a soaking time of 120 min almost all of the particles became Ca-α sialon hollow balls composed of nanosized particles (Fig. 3(c)). The XRD result shows some Ca-α sialon and AlN peaks in the product after 30 min, and a phase composition of 85 wt% Ca-α sialon and 15 wt% AlN was determined for the final product fired at 1450°C for 120 min. Quantitative phase analysis was performed using the relative peak intensities of α-sialon and AlN. Hence, the morphological change from solid to hollow balls and the formation of Ca-α sialon took place simultaneously.

A FESEM micrograph of a spherical particle obtained at 1450°C after 0 min is shown in Fig. 4. It was found that very fine particles (>50 nm) were formed on the surface of the solid balls at the initial stage of CRN. These fine particles may act as nuclei from which nanosized Ca-α sialon particles can subsequently grow.

Figure 5 presents typical EDS spectra from the ball-shaped particles formed at 1450°C after 0 min. EDS analysis indicates that the solid balls have a chemical composition of Si, Al, Ca, O and a small amount of N, and all solid balls have a nearly uniform composition. The existence of N in the spectrum suggests that the nitridation reaction has started when the solid balls are formed, and it also supports the identification of oxynitride phases such as Si_2N_2O and $SiAl_7O_2N_7$ by XRD at this temperature. Additional electron diffraction analysis of the solid balls shows only the amorphous halo, confirming that the

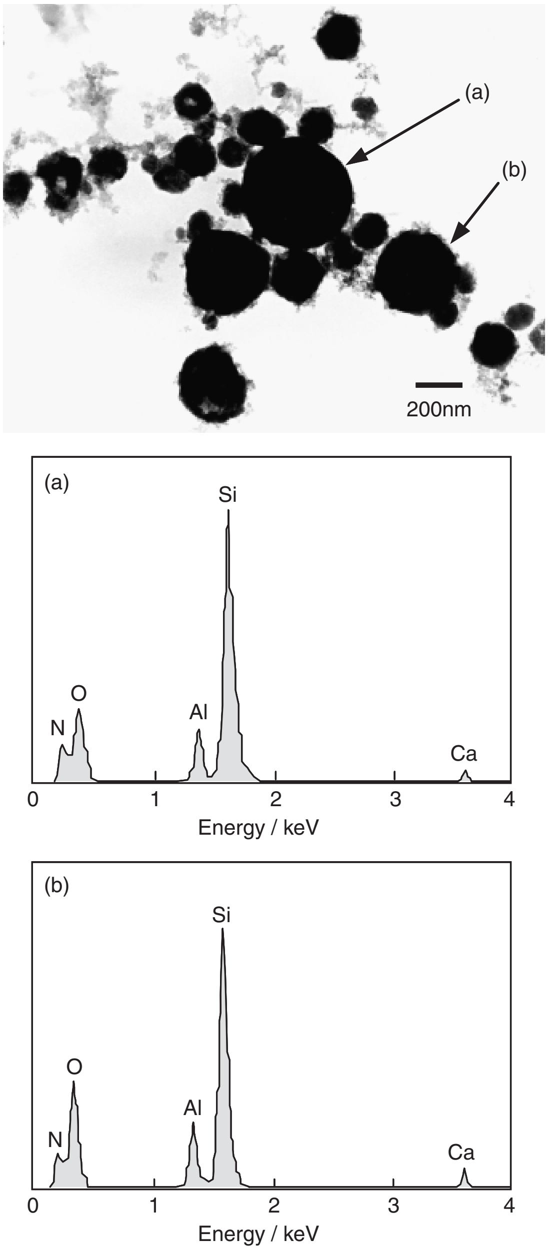

Fig. 5. Typical energy-dispersive spectrometry spectra of the products fired at 1450°C for 0 min in N_2 flow.

solid balls at the initial stage of CRN are mainly a Si–Al–Ca–O amorphous phase.

Based on the above observations, the formation process of Ca-α sialon hollow balls is proposed in Fig. 6. When the heating temperature for raw powders was increased, the interaction of SiO_2, Al_2O_3, and CaO (from the decomposition of $CaCO_3$) particles resulted in local melting, probably above 1000°C. Further increasing the temperature, ball-shaped particles consisting of a Si–Al–Ca–O liquid phase were formed and coated by fine carbon particles on the surface. Hence, carbon particles, in addition to acting as a reducing agent, seem to play a significant role in the formation of the spherical particles. With increasing time and temperature, nitrogen diffused into the liquid to form nitrogen-containing Si–Al–Ca–O balls. The interfacial tension at the liquid/carbon interface decreased with increasing temperature, but the viscosity of the liquid phase increased with doping by N,[28] resulting in the ball shape of the particles remaining unchanged. With extension of time at 1450°C, CRN proceeded further, resulting in the formation of fine α-sialon on the surface of the spherical particles. The conversion from an amorphous Si–Al–Ca–O–N phase to crystalline α-sialon is accompanied by an increase in density due to lattice ordering and a decrease in mass due to replacement of O by N. The increase in density on the surface requires material to be drawn from the interior of the ball to the surface, thereby producing the hollow Ca-α sialon ball shape.

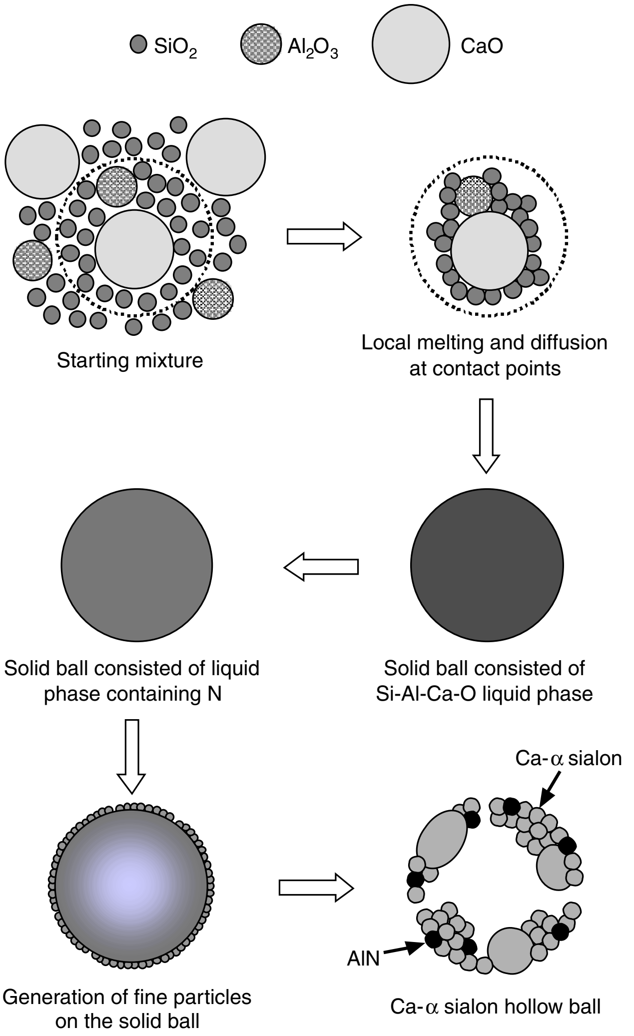

Fig. 6. Schematics of the suggested formation process for Ca-α sialon hollow balls.

We have already performed experiments to synthesize α-sialon powders in different compositions, including Mg and rare-earth oxides. The solid- and hollow-ball morphologies were not observed in the MgO–SiO_2–Al_2O_3 system. In the Y, Yb, Sm, Nd, and Dy systems, a small number of hollow balls were observed in the specimens fired at 1450°C for 120 min. Meanwhile, solid-ball particles were also observed in these systems at 1450°C after 0 min. However, compared with the Ca system, the

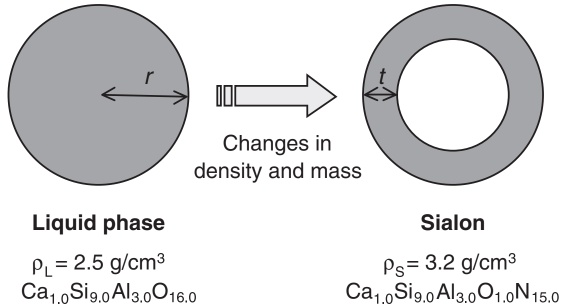

Fig. 7. Illustration of the estimation of thickness of the hollow-ball shell. ρ_L and ρ_S are the densities of liquid phase and sialon, respectively.

amount of solid balls was much less and the ball shape was not clear. In the Y_2O_3–SiO_2–Al_2O_3 system, SEM observation showed some spherical particles formed at 1400°C. The eutectic temperature for the Y_2O_3–SiO_2–Al_2O_3 system is about 1350°C.[29] The spherical particles were considered to be produced through a Si–Al–Y–O liquid phase as in the CaO–SiO_2–Al_2O_3 system. The viscosity of the liquid phase in the MgO–SiO_2–Al_2O_3 system is lower than that in the CaO–SiO_2–Al_2O_3 system.[30] Moreover, the eutectic temperature for the MgO–SiO_2–Al_2O_3 system is 1350°C,[31] which is higher than that of the CaO–SiO_2–Al_2O_3 system. Hence, the solid balls were assumed not to form in the Mg–Si–Al–O system at the initial stage of the nitridation because of the low viscosity, and thus the hollow balls were not finally observed. Also, the eutectic temperature for the Y_2O_3–SiO_2–Al_2O_3 system is higher than that for the CaO–SiO_2–Al_2O_3 system. It may be difficult to form a large number of solid and hollow balls in the rare-earth systems, such as Y_2O_3–SiO_2–Al_2O_3, because the viscosity of the liquid phases in these systems may be too high at the CRN temperature of 1450°C.

When the accompanying changes in both density and mass are taken into consideration, the thickness of the hollow-ball shell after conversion from a solid ball can be estimated (Fig. 7).

Concerning the change in mass, the loss in mass M can be described as

$$M = 1 - \frac{W_S}{W_L} = 1 - \frac{\frac{4}{3}\pi\left[r^3 - (r-t)^3\right]\rho_S}{\frac{4}{3}\pi r^3 \rho_L} \qquad (2)$$

where W_L and W_S are weights of the liquid phase and the sialon, respectively, r is radius of the liquid sphere, t is thickness of the hollow-ball shell of sialon, ρ_L and ρ_S are densities of the liquid phase and the sialon, respectively, and M is loss in mass. Rearranging Eq. (2), we obtain

$$\frac{t}{r} = 1 - \left[1 - \frac{\rho_L}{\rho_S}(1-M)\right]^{\frac{1}{3}} \qquad (3)$$

The decrease in mass M owing to replacement of O by N, that is the conversion from $Ca_{1.0}Si_{9.0}Al_{3.0}O_{16.0}$ to $Ca_{1.0}Si_{9.0}Al_{3.0}O_{1.0}N_{15.0}$, is 5%. In the case of $\rho_L = 2.5$ g/cm^3 and $\rho_S = 3.2$ g/cm^3,[30,32] substituting these values into Eq. (3) gives a calculated value of $t/r = 0.36$. The diameter of solid balls, $2r$, is 200–500 nm in this study. Therefore, when the diameter equals 200–500 nm, the shell thickness is 36 and 90 nm, respectively. Assuming that the diameter of both solid and hollow balls is unchanged after the conversion, this calculation indicates that the hole in the center is very large and the shell consists of single to triple α-sialon particles of ~30 nm, as seen in our previous report.[23]

IV. Conclusions

The formation process of Ca-α sialon hollow balls in the SiO_2–Al_2O_3–CaO system was analyzed by investigating the products of CRN formed at various stages during the CRN sequence. A large number of solid-ball particles consisting of a Si–Al–Ca–O amorphous phase were formed at the initial stage of CRN. Very fine particles were subsequently generated on the surface of these solid balls, which gradually changed into hollow balls with continuing nitridation reaction. An increase in density and a decrease in mass are the results of the conversion from the amorphous sphere to crystalline α-sialon, which are responsible for the formation of Ca-α sialon hollow balls composed of nanosized particles.

Acknowledgments

The authors thank Mr. Y. Shimada (Yokohama National University) for the TEM and EDS investigations and Dr. Y. Yoshizawa (AIST, Japan) for the FESEM observation.

References

[1] C. A. Wood, H. Zhao, and Y.-B. Cheng, "Microstructural Development of Calcium α-SiAlON Ceramics with Elongated Grains," *J. Am. Ceram. Soc.*, **82** [2] 421–8 (1999).

[2] C. L. Hewett, Y.-B. Cheng, B. C. Muddle, and M. B. Trigg, "Phase Relationships and Related Microstructural Observations in the Ca–Si–Al–O–N System," *J. Am. Ceram. Soc.*, **81** [7] 1781–8 (1998).

[3] C. L. Hewett, Y.-B. Cheng, B. C. Muddle, and M. B. Trigg, "Thermal Stability of Calcium α-Sialon Ceramics," *J. Eur. Ceram. Soc.*, **18**, 417–27 (1998).

[4] I.-W. Chen and A. Rosenflanz, "A Tough SiAlON Ceramics Based on α-Si_3N_4 with a Whisker-Like Microstructure," *Nature (London)*, **389**, 701–4 (1997).

[5] J. Tatami, M. Iguchi, M. Hotta, C. Zhang, K. Komeya, T. Meguro, M. Omori, T. Hirai, M. E. Brito, and Y.-B. Cheng, "Fabrication and Evaluation of Ca-α SiAlON Nano Ceramics," *Key Eng. Mater.*, **237**, 105–10 (2003).

[6] H. Zhao, S. P. Swenser, and Y.-B. Cheng, "Elongated α-Sialon Grains in Pressureless Sintered Sialon Ceramics," *J. Eur. Ceram. Soc.*, **18**, 1053–7 (1998).

[7] K. H. Jack, "Review: SiAlONs and Related Nitrogen Ceramics," *J. Mater. Sci.*, **11**, 1135–58 (1976).

[8] J.-G. Lee and I. B. Culter, "Sinterable SiAlON Powder by Reaction of Clay with Carbon and Nitrogen," *Am. Ceram. Soc. Bull.*, **58**, 869–71 (1979).

[9] H. Yoshimatsu, M. Mitomo, H. Mihashi, S. Ohmori, and T. Yabuki, "The Preparation of Sialon Powder from Kaolinite (in Japanese)," *J. Ceram. Soc. Jpn.*, **91**, 442–9 (1983).

[10] H. Yoshimatsu, T. Yabuki, and H. Mihashi, "Preparation of Sialon Powder from Mixture of SiO_2 and $Al_2O_3 \cdot 2H_2O$ by Thermal Carbon Reduction (in Japanese)," *J. Ceram. Soc. Jpn.*, **95**, 590–4 (1987).

[11] M. Sopicka-Lizer, R. A. Terpstra, and R. Metselaar, "Carbothermal Production of β-Sialon from Alumina, Silica and Carbon Mixture," *J. Mater. Sci.*, **30**, 6363–9 (1995).

[12] M. Mitomo, T. Shiogai, H. Yoshimatsu, and Y. Kitami, "Preparation of Sialon Powder from Alkoxides (in Japanease)," *J. Ceram. Soc. Jpn.*, **93**, 364–9 (1985).

[13] O. Yamamoto, M. Ishida, Y. Saitoh, T. Sasamoto, and S. Shimada, "Influence of Mg^{2+} on the Formation of β-SiAlON by the Carbothermal Reduction–Nitridation of Homogeneous Gel," *Int. J. Inorg. Mater.*, **3**, 715–9 (2001).

[14] Q. Li, C. Zhang, K. Komeya, J. Tatami, T. Meguro, and L. Gao, "Nano Powders of β-Sialon Carbothermally Produced via a Sol–Gel Process," *J. Mater. Sci. Lett.*, **22**, 885–7 (2003).

[15] F. J. Li, J. Tatami, T. Meguro, and K. Komeya, "Synthesis of β-SiAlON Powder by Carbothermal Reduction–Nitridation," *Key Eng. Mater.*, **247**, 109–12 (2003).

[16] M. Mitomo, M. Takeuchi, and M. Ohmasa, "Preparation of α-Sialon Powders by Carbothermal Reduction and Nitridation," *Ceram. Int.*, **14**, 43–8 (1988).

[17] J. W. T. van Rutten, R. A. Terpstra, J. C. T. Heijde, H. T. Hintzen, and R. Metselaar, "Carbothermal Preparation and Characterisation of Ca–α-Sialon," *J. Eur. Ceram. Soc.*, **15**, 599–604 (1995).

[18] T. Ekström, Z.-J. Shen, K. J. D. MacKenzie, I. W. M. Brown, and G. V. White, "α-Sialon Ceramics Synthesised from a Clay Precursor by Carbothermal Reduction and Nitridation," *J. Mater. Chem.*, **8**, 977–83 (1998).

[19] C. Zhang, K. Komeya, J. Tatami, T. Meguro, and Y.-B. Cheng, "Synthesis of Mg-α SiAlON Powders from Talc and Halloysite Clay Minerals," *J. Eur. Ceram. Soc.*, **20**, 1809–14 (2000).

[20] J. Y. Qiu, J. Tatami, C. Zhang, K. Komeya, T. Meguro, and Y.-B. Cheng, "Influence of Starting Material Composition and Carbon Content on the Preparation of Mg–α SiAlON Powders by Carbothermal Reduction–Nitridation," *J. Eur. Ceram. Soc.*, **22**, 2989–96 (2002).

[21] Y.-B. Cheng, M. R. Terner, W. W. Chen, and P. L. Wang, "Slag Derived α-Sialon Ceramics and their Properties," *Key Eng. Mater.*, **264–268**, 781–6 (2004).

[22] M. R. Terner and Y.-B. Cheng, "Densification and High Temperature Stability of Low-Cost α-Sialons Derived from Slag via Carbothermal Reduction–Nitridation," *Proc. Int. Conf. Adv. Mat. Proc 3, Melbourne 2004*, 50–1 (2004).

[23] K. Komeya, C. Zhang, M. Hotta, J. Tatami, T. Meguro, and Y.-B. Cheng, "Hollow Beads Composed of Nanosize Ca α-SiAlON Grains," *J. Am. Ceram. Soc.*, **83** [4] 995–7 (2000).

[24] J. Tatami, T. Ohta, C. Zhang, M. Hotta, K. Komeya, T. Meguro, M. Omori, and T. Hirai, "Fabrication and Evaluation of Porous Ca–α SiAlON Ceramics," *Ceram. Trans.*, **142**, 77–87 (2003).

[25] I. H. Kang, K. Komeya, T. Meguro, M. Naito, and O. Hayakawa, "Effect of Silicon Nitride Seeds Addition on the Particle Size and the Crystal Form of Resulting Powder in Carbothermal Reduction–Nitridation of Silica," *J. Ceram. Soc. Jpn.*, **104**, 471–5 (1996).

[26] R. A. L. Drew, *Nitrogen Glass.* The Parthenon Press, Casterton Hall, UK, 1986.

[27] E. M. Levin, C. R. Robbins, and H. F. McMurdie, "Fig. 630"; p. 219 in *Phase Diagrams for Ceramists*, Edited by M. K. Reser. American Ceramic Society, Columbus, OH, 1964.

[28] S. Sakka, K. Kamiya, and T. Yoko, "Preparation and Properties of Ca–Al–Si–O–N Oxynitride Glasses," *J. Non-Crystal. Solids*, **56**, 147–52 (1983).

[29] E. M. Levin, C. R. Robbins, and H. F. McMurdie, "Fig. 2586"; p. 165 in *Phase Diagrams for Ceramists*, Edited by M. K. Reser. American Ceramic Society, Columbus, OH, 1969.

[30] O. V. Mazurin, M. V. Streltsina, and T. P. Shvaiko-shvaikovskaya, *Physical Science Data 15, Handbook of Glass Data, Part C, Ternary Silicate Glasses.* Elsevier, New York, 1987.

[31] E. M. Levin, C. R. Robbins, and H. F. McMurdie, "Fig. 712"; p. 246 in *Phase Diagrams for Ceramists*, Edited by M. K. Reser. American Ceramic Society, Columbus, OH, 1964.

[32] JCPDS, International Centre for Diffraction Data, No.33–261. □